Bioorganic Chemistry 104 (2020) 104235

Contents lists available at ScienceDirect

Bioorganic Chemistry

journal homepage: www.elsevier.com/locate/bioorg

Synthesis and biological study of class I selective HDAC inhibitors with NO releasing activity

Qin'ge Ding[a,1], Chunxi Liu[b,1], Chunlong Zhao[a], Hang Dong[a], Qifu Xu[a], C. James Chou[c], Yingjie Zhang[a,*]

[a] Department of Medicinal Chemistry, Key Laboratory of Chemical Biology (Ministry of Education), School of Pharmaceutical Sciences, Cheeloo College of Medicine, Shandong University, 44 West Wenhua Road, Ji'nan, Shandong 250012, PR China
[b] Department of Pharmacy, Qilu Hospital, Cheeloo College of Medicine, Shandong University, Ji'nan, Shandong 250012, PR China
[c] Department of Drug Discovery and Biomedical Sciences, South Carolina College of Pharmacy, Medical University of South Carolina, Charleston, SC 29425, United States

ARTICLE INFO

Keywords:
Histone deacetylase
Nitric oxide
Hybrid
Anticancer
Phenylsulfonylfuroxan
N-acyl-*o*-phenylenediamine

ABSTRACT

Based on the multi-mechanism antitumor strategy and the regulatory effect of nitric oxide (NO) on histone deacetylases (HDACs), a series of *N*-acyl-*o*-phenylenediamine-based HDAC inhibitors equipped with the phenylsulfonylfuroxan module as NO donor was designed, synthesized and biologically evaluated. The in vitro HDAC inhibitory assays revealed that compared with the clinical class I selective HDAC inhibitor MS275, compounds **7c**, **7d** and **7e** possessed similar HDAC inhibitory potency and selective profile, which were confirmed by the results of western blot analysis. The western blot analysis also showed that NO scavenger *N*-acetyl cysteine (NAC) could weaken the intracellular HDAC inhibitory ability of compound **7c**, supporting the HDAC inhibitory effect of NO generated by **7c**. It is worth noting that compounds **7c**, **7d** and **7e** exhibited more potent in vitro antiproliferative activities than MS275 against all four tested solid tumor cell lines. The promising in vivo antitumor potency of **7c** was demonstrated in a HCT116 xenograft model.

1. Introduction

Histone deacetylases (HDACs), a family of enzymes, play important roles in epigenetic regulation and post-translational modification by removing the acetyl groups from histones and non-histone proteins [1]. Recently, HDACs have been extensively investigated as anticancer targets. To date, four pan-HDAC inhibitors (vorinostat, belinostat, panobinostat, romidepsin, Fig. 1) have received approval in the United States for the treatment of cutaneous T cell lymphoma, peripheral T cell lymphoma or multiple myeloma. In addition, a class I selective HDAC inhibitor chidamide (Fig. 1) has been approved in China for use in patients with peripheral T cell lymphoma [2]. Despite the success in treating hematologic malignancies, most HDAC inhibitors showed limited efficacy as monotherapy against solid tumors. Noteworthily, HDAC inhibitor-based drug combination or multi-target/multi-mechanism agent offers hope to conquer this problem [3–5]. Compared with drug combination, multi-target/multi-mechanism agents show advantages in more predictable pharmacokinetic profiles, less drug-drug interaction and better patient compliance [6–8], despite of the possible larger molecular weights and more complex synthesis.

Nitric oxide (NO), an endogenous signal or effector molecule, accounts for various important cellular functions including vasodilation, neurotransmission, cell migration, immune response and apoptosis [9]. There has been accumulating evidence suggesting that high concentrations of NO can exhibit multiple antitumor effects, therefore NO donors have been researched and developed as potential antitumor agents [10–12]. Two phase II clinical trials demonstrated that NO donor nitroglycerin combined with chemotherapy may improve overall response, progression-free survival or time to disease progression in patients with non-small cell lung cancer [13,14]. Moreover, one small molecular compound named RRx-001 with NO releasing activity is currently in phase I/II clinical trials for cancer therapy [15,16].

Intriguingly, there were research revealing that NO could lead to S-nitrosylation modification of HDAC2 in neurons, inducing the release of HDAC2 from chromatin and the subsequent hyperacetylation of histones and gene activation [17,18]. Another research demonstrated that NO could inhibit the deacetylase activity of HDAC2 and HDAC1 by S-nitrosylation-dependent and independent mechanism, respectively [19]. Taken together, it is suggested that NO could negatively regulate the biological function of many HDACs, at least the class I isoforms of

* Corresponding author.
E-mail address: zhangyingjie@sdu.edu.cn (Y. Zhang).
[1] These two authors contributed equally.

https://doi.org/10.1016/j.bioorg.2020.104235
Received 30 June 2020; Received in revised form 4 August 2020; Accepted 12 August 2020
Available online 26 August 2020
0045-2068/

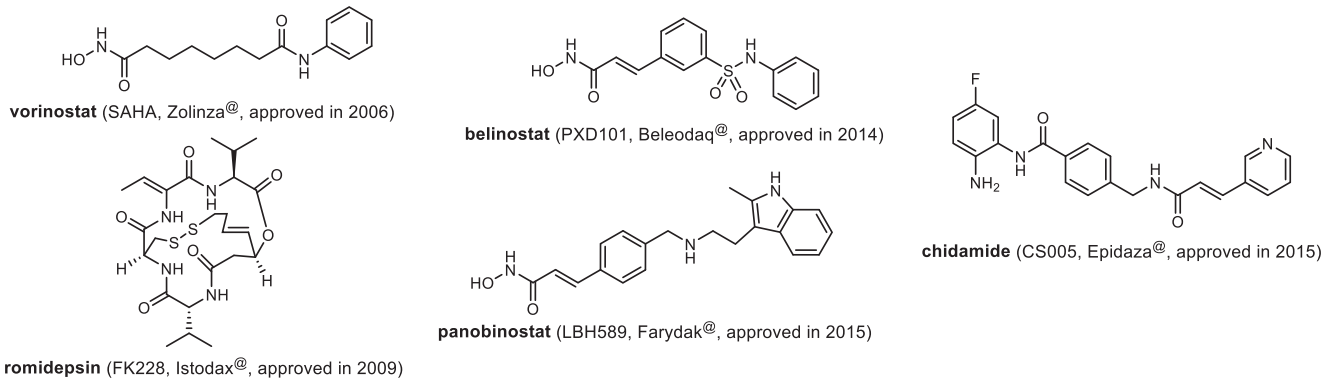

Fig. 1. The structures of approved anticancer HDAC inhibitors.

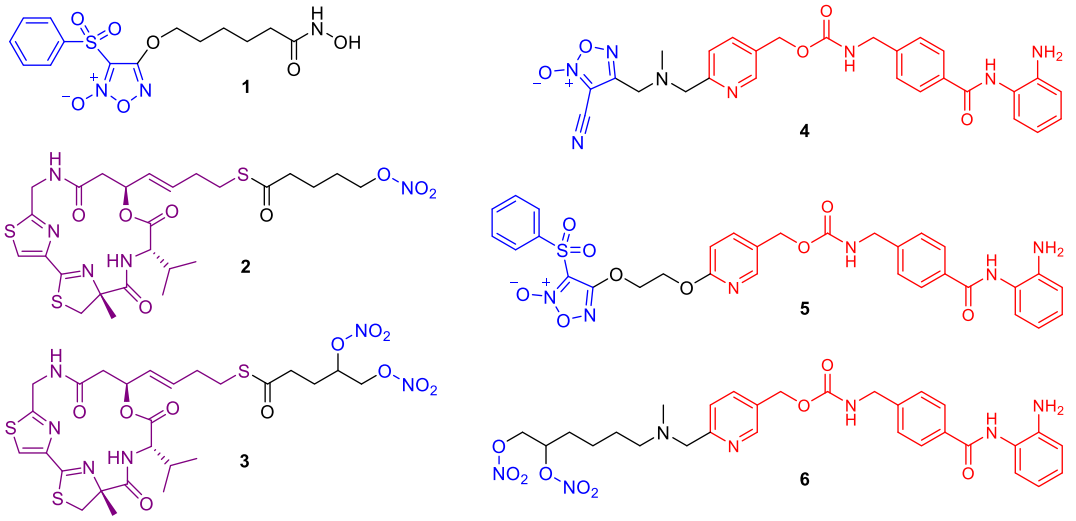

Fig. 2. The structures of reported hybrid molecules of HDAC inhibitor and NO donor. The NO donors are indicated in blue, the functional part of Largazole targeting HDAC is indicated in purple, and the structure of MS275 is indicated in red. (For interpretation of the references to colour in this figure legend, the reader is referred to the web version of this article.)

HDAC2 and HDAC1. Therefore, hybrid molecules of HDAC inhibitor and NO donor is supposed to possess more potent HDAC inhibitory and antitumor activity than common HDAC inhibitors. In our previous research, a novel series of hydroxamate-based HDAC inhibitors with a phenylsulfonylfuroxan module as the NO donor was designed and synthesized, among which compound **1** (Fig. 2) exhibited superior HDAC inhibitory activity, in vitro and in vivo antitumor potency relative to the approved HDAC inhibitor vorinostat [20]. Lately, two Largazole analogs as dual HDAC inhibitor and NO donors (compounds **2** and **3**, Fig. 2) were developed, which also showed promising in vitro antitumor potency [21]. In addition, several hybrids of HDAC inhibitor MS275 and NO donor (compounds **4**, **5** and **6**, Fig. 2) were developed as muscle differentiation agents, while no antitumor activity was reported [22,23].

In the present research, a novel HDAC inhibitor-NO donor hybrid **7c** was designed and synthesized based on the structure of our previously reported compound **1** (Fig. 3). The main purpose of structural modification of compound **1** was to get the analogs with improved HDAC isoform selectivity, given that the *N*-acyl-*o*-phenylenediamine group could generally afford class I selective HDAC inhibitors [2]. Structure-activity relationship (SAR) study was focused on the linker part of compound **7c**, leading to a series of hybrids of *N*-acyl-*o*-phenylenediamine and phenylsulfonylfuroxan (Fig. 3). Among these hybrids, three analogs **7c**, **7d** and **7e** exhibited not only potent HDAC1/2/3 inhibitory activities but also significant NO releasing capabilities, which contributed to the remarkable in vitro antiproliferative potency against

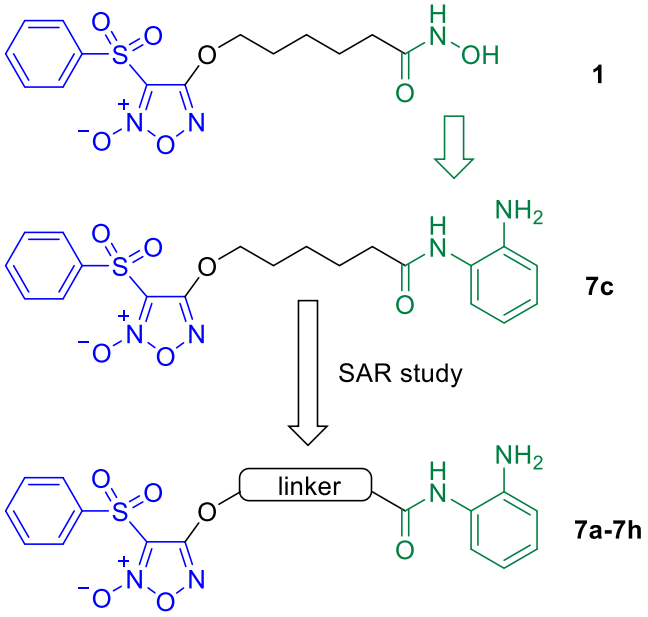

Fig. 3. Design strategy of the target compounds.

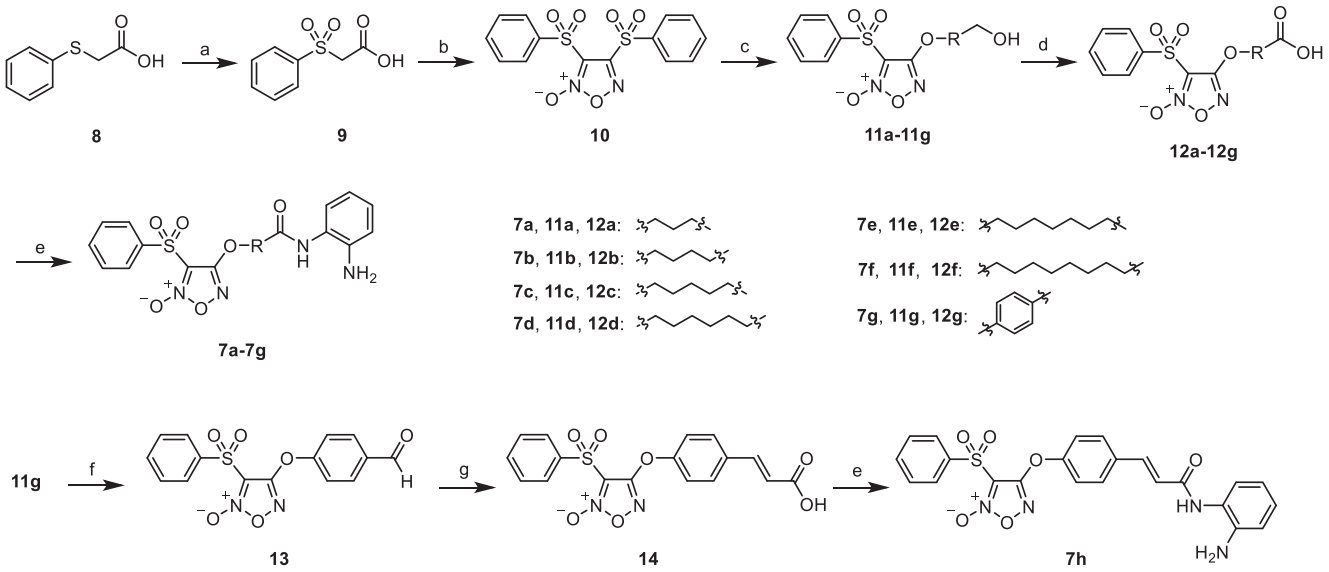

Scheme 1. Synthesis of compounds **7a-7h**. Reagents and conditions: (a) H_2O_2, CH_3COOH; (b) conc. HNO_3; (c) HO-R-CH_2-OH, 25%NaOH; (d) *Jones* agent, acetone; (e) TBTU, TEA, THF; *o*-phenylenediamine. (f) PCC, DCM, 0°C; (g) propandioic acid, pyrrolidine, pyridine, reflux.

both hematological and solid tumor cell lines. Additionally, the in vivo antitumor activity of compound **7c** in a HCT116 xenograft model was comparable to, if not better than that of MS275, a class I selective HDAC inhibitor in clinical trials.

2. Results and discussion

2.1. Chemistry

The synthesis of target compounds **7a-7h** was described in Scheme 1. Oxidization of the starting material **8** by H_2O_2 led to compound **9**. Without separation and purification, compound **9** was further progressed to one-pot reaction with fuming HNO_3 to get compound **10**. Substitution of **10** with corresponding dihydroxy compounds led to alcohols **11a-11g**, which were oxidized to carboxylic acids **12a-12g**, respectively. The target compounds **7a-7g** were obtained by condensation of **12a-12g** with *o*-phenylenediamine. The intermediate alcohol **11 g** could also be oxidized by PCC to get aldehyde **13**. Subsequent reaction with propandioic acid and condensation with *o*-phenylenediamine afforded the target compound **7h**.

2.2. In vitro HDACs inhibitory assay

HeLa cell nuclear extract (mainly contains HDAC1 and 2) was used to preliminarily evaluate the HDAC inhibitory potency of the target compounds with the clinical HDAC inhibitor MS275 as the positive control. The results in Table 1 showed that all newly synthesized hybrids exhibited moderate to potent total HDAC inhibitory activities against HeLa cell nuclear extract, with compounds **7c** (IC_{50} = 2.16 ± 0.26 μM), **7d** (IC_{50} = 1.69 ± 0.42 μM) and **7e** (IC_{50} = 2.51 ± 0.27 μM) being comparable to MS275 (IC_{50} = 1.56 ± 0.17 μM). For analogs with aliphatic linkers (**7a-7f**), their HDAC inhibitory activities first increased then decreased with the linker length, culminating in compound **7d** (IC_{50} = 1.69 ± 0.42 μM). Compounds **7g** and **7h** with aromatic linkers showed much less potent HDAC inhibitory activities than compounds with aliphatic linkers (**7a-7f**). The inferior activities of **7g** and **7h** could be ascribed to their aromatic linkers, which might be too rigid to fit in the active site of HDAC.

Table 1
Total HDAC inhibitory activities of compounds **7a-7h.**

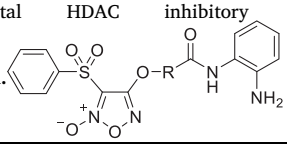

Compd	R	IC_{50} (μM)[a] HeLa nuclear extract
7a		14.3 ± 2.1
7b	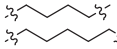	8.01 ± 1.54
7c	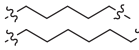	2.16 ± 0.26
7d	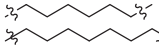	1.69 ± 0.42
7e	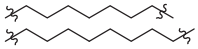	2.51 ± 0.27
7f	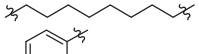	14.9 ± 3.4
7g		30.5 ± 3.7
7h	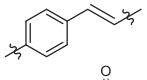	27.5 ± 2.9
MS275	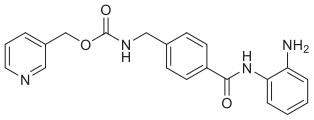	1.56 ± 0.17

[a] Assays were performed in replicate (n ≥ 3), values are shown as mean ± SD.

Table 2
HDAC isoform selectivity of compounds **7c**, **7d**, **7e** and MS275.

Compd	IC_{50} (μM)[a]				
	Class I			Class IIa	Class IIb
	HDAC1	HDAC2	HDAC3	HDAC4	HDAC6
7c	0.62 ± 0.14	1.46 ± 0.24	0.62 ± 0.14	> 10	> 10
7d	0.47 ± 0.11	1.14 ± 0.18	0.56 ± 0.13	> 10	> 10
7e	0.66 ± 0.17	1.20 ± 0.26	0.52 ± 0.14	> 10	> 10
MS275	0.16 ± 0.03	0.40 ± 0.07	0.61 ± 0.11	> 10	> 10

[a] Assays were performed in replicate (n ≥ 3), values are shown as mean ± SD.

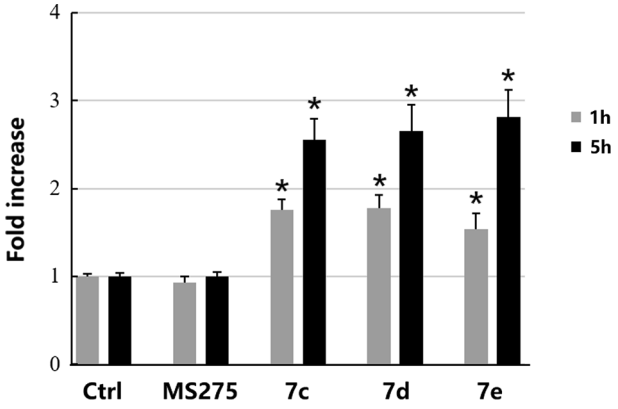

Fig. 4. NO production of compounds in HeLa cells. Data are represented as means ± SD obtained from at least three independent experiments. * $p < 0.05$ versus the control groups by Student's two-tailed *t* test.

2.3. In vitro HDACs isoform selectivity assay

Considering their potent total HDAC inhibitory activities, compounds **7c**, **7d** and **7e** were further tested in HDAC isoform selectivity assay. Their IC_{50} values against three class I isoforms (HDAC1, HDAC2 and HDAC3), one class IIa isoform (HDAC4) and one class IIb isoform (HDAC6) were determined and compared with MS275 (Table 2). As expected, all *N*-acyl-*o*-phenylenediamine-based compounds were class I selective but showed no significant preference among different class I isoforms. In general, compared with MS275, the HDAC1 and HDAC2 inhibitory activities of **7c**, **7d**, **7e** were slightly less potent, while their HDAC3 inhibitory activities were quite similar.

2.4. In vitro NO release assay

The NO releasing capabilities of compounds **7c**, **7d** and **7e** were characterized in HeLa cells, which were incubated with different compounds (10 μM) for 1 h or 5 h. After incubation, the intracellular levels of NO were measured using the Griess method, which measures the nitrate/nitrite levels to quantify the NO released [24]. As shown in Fig. 4, compounds **7c**, **7d** and **7e** bearing the phenylsulfonylfuroxan moiety could effectively release NO in a time dependent manner, represented as fold increase based on the control group with endogenous nitrate/nitrite. In contrast, MS275 displayed no NO releasing capability, which was in line with the literature results [22,23].

2.5. Western blot analysis

With confirmed HDAC inhibitory activity and NO donating capability, one representative compound **7c** was progressed to western blot analysis to investigate their intracellular target engagement. The results in Fig. 5A showed that both MS275 and **7c** could dramatically increase the intracellular levels of the class I HDAC substrate acetyl-histone H4 (ac-HH4) without influencing the HDAC6 substrate acetyl-α-tubulin (ac-α-tub). This was in line with the HDAC isoform selective profiles shown in Table 2. Besides, we performed another set of western blot analysis to investigate if NO generated by **7c** contributed to its intracellular HDAC inhibition. As we can see in Fig. 5B, NO scavenger *N*-acetyl cysteine (NAC) could significantly compromise the class I HDAC inhibitory activity of **7c** while showed no influence on MS275, confirming the HDAC inhibitory effect of NO as previously reported [17–19].

2.6. In vitro anti-proliferative assay

Considering their potent HDAC inhibitory and NO donating activities, compounds **7c**, **7d** and **7e** were evaluated for their anti-proliferative activities against three hematological tumor cell lines and four solid tumor cell lines. MS275 was used as the positive control. According to the results in Table 3, all compounds could attenuate tumor cell growth effectively. Typically, HDAC inhibitors are more cytotoxic to hematological cell lines than solid tumor cell lines. This trend was also observed in MS275 and hybrids **7c**, **7d** and **7e**. For the three tested hematological tumor cell lines, **7c**, **7d** and **7e** were more potent against the human erythroleukemia cell line HEL, but less potent against the human acute lymphoblastic leukemia cell line MOLT-4 and the human acute *T*-cell leukemia cell line Jurkat than MS275. On the whole, the anti-hematological malignancy potency of our hybrid compounds was comparable to that of MS275. It was worth noting that hybrids **7c**, **7d** and **7e** exhibited more potent activities against all tested solid tumor cell lines than MS275. Among the four tested solid tumor cell lines, the human colon cancer cell line HCT116 showed the most sensitivity to our hybrid compounds, which possessed IC_{50} values against HCT116 lower than 1 μM.

2.7. In vivo antitumor evaluation

Finally, a HCT116 xenograft model in nude mice was established to evaluate the in vivo antitumor potency of the representative compound **7c** with MS275 as the positive control. On the basis of our previous research, oral administration of MS275 in the dosage of 50 mg/kg/d was effective but toxic in xenograft models [25]. Therefore, in the present research the dosage of MS275 was reduced to 30 mg/kg/d. To better compare the in vivo antitumor potency of **7c** and MS275, the dosage of **7c** was also set as 30 mg/kg/d. After 15 consecutive days of treatment, tumor growth inhibition (TGI) and relative increment ratio (T/C) were calculated to evaluate the antitumor effects in the aspects of tumor weight and tumor volume, respectively. As shown in Table 4, compound **7c** exhibited potent in vivo antitumor efficacy, which was comparable to, if not better than that of MS275 at the same dosage. The tumor growth curve was presented in Fig. 6. Moreover, mice treated by **7c** showed no significant body weight loss (Fig. 7), suggesting the acceptable toxicity of **7c**.

3. Conclusion

In summary, a novel series of *N*-acyl-*o*-phenylenediamine-based

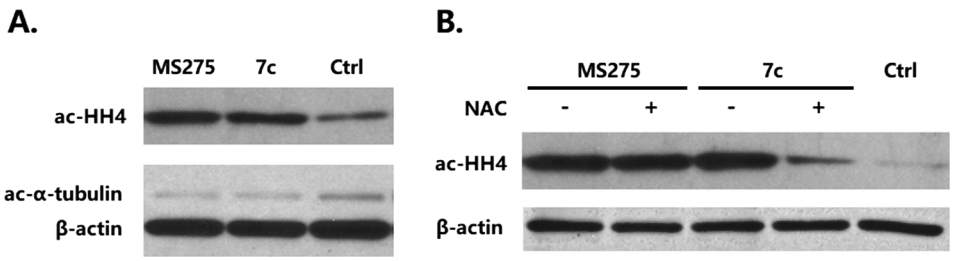

Fig. 5. (**A**) HeLa cells were treated with compounds (2 μM) or DMSO for 5 h. (**B**) HeLa cells were preincubated with 10 μM of NAC, then were treated with 2 μM of MS275 or **7c** for 5 h. The levels of ac-α-tub and ac-HH4 were determined by immunoblotting. β-Actin was used as a loading control.

Table 3
In *vitro* anti-proliferative activity of compounds **7c**, **7d**, **7e** and MS275.

Cpd	IC_{50} (μM)[a]						
	Hematological tumor cell lines			Solid tumor cell lines			
	HEL	MOLT-4	Jurkat	HeLa	PC-3	HCT116	A549
7c	0.32 ± 0.06	0.59 ± 0.09	0.54 ± 0.05	1.23 ± 0.06	2.69 ± 0.15	0.93 ± 0.08	1.03 ± 0.09
7d	0.41 ± 0.05	0.54 ± 0.02	0.77 ± 0.12	1.50 ± 0.11	2.50 ± 0.10	0.77 ± 0.06	0.98 ± 0.06
7e	0.42 ± 0.05	0.72 ± 0.15	0.47 ± 0.07	1.56 ± 0.11	1.92 ± 0.09	0.79 ± 0.09	1.55 ± 0.03
MS275	0.68 ± 0.07	0.46 ± 0.02	0.25 ± 0.03	3.36 ± 0.22	9.67 ± 1.62	1.64 ± 0.22	2.05 ± 0.14

[a] Assay were performed in replicate (n ≥ 3), values are shown as mean ± SD.

Table 4
In vivo antitumor efficacy of compounds **7c** and MS275 in the HCT116 xenograft mode.

Compd	Administration	T/C (%)[a]	TGI (%)[a]
7c	30 mg/kg/d, PO	57	36
MS275	30 mg/kg/d, PO	64	31

[a] Compared with the control group, all treated groups showed statistically significant ($P < 0.05$) T/C and TGI by Student's two-tailed *t* test.

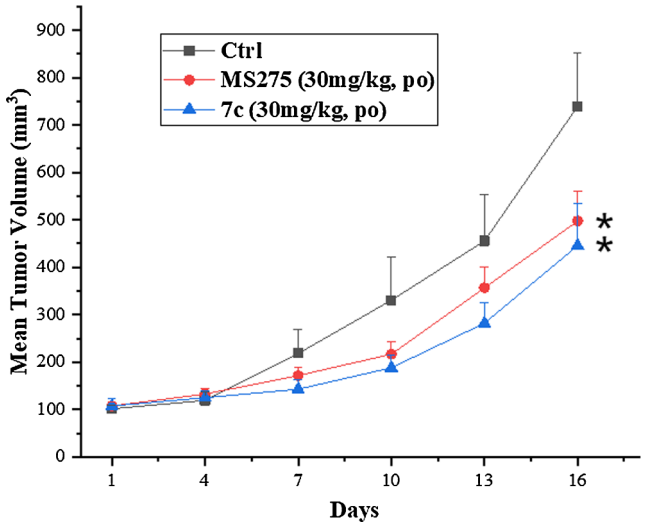

Fig. 6. Growth curve of implanted HCT116 xenograft in nude mice. Data are expressed as the mean ± SD. * $p < 0.05$ versus the control groups by Student's two-tailed *t* test.

HDAC inhibitors equipped with the phenylsulfonylfuroxan module was designed, synthesized and biologically evaluated. Among these analogs, three compounds (**7c**, **7d** and **7e)** with aliphatic linkers of suitable length (4–6 methylene groups) showed remarkable inhibition and selectivity towards class I HDACs. The NO donating activities of these three analogs were validated using the Griess method. The intracellular class I HDAC inhibitory potency and selectivity of one representative compound **7c** were validated by western blot analysis, which also revealed that NO generated by **7c** also contributed to its intracellular HDAC inhibition. The dual biological activities endowed compounds **7c**, **7d** and **7e** with considerable in vitro antiproliferative potencies, especially against the solid tumor cell lines. The results of xenograft experiment presented the favorable in vivo antitumor potency and toxic profile of **7c**, which supported its further research and development as a novel antitumor agent.

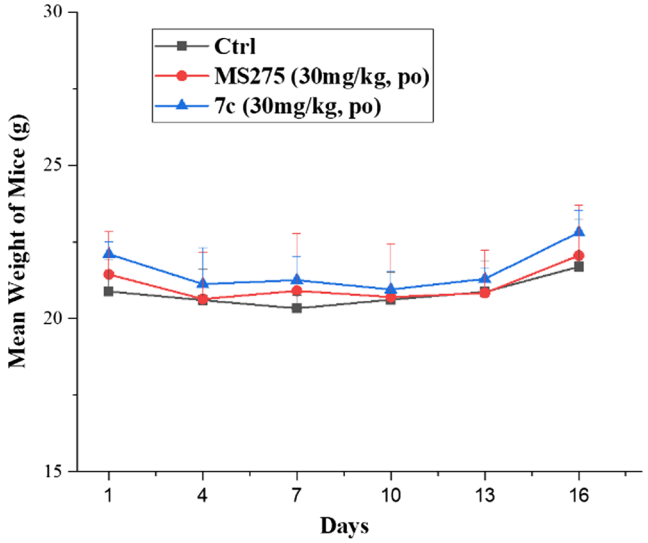

Fig. 7. Body weight curve of nude mice. Data are expressed as the mean ± SD.

4. Experimental section

4.1. Chemistry

Unless specified otherwise, all starting materials, reagents and solvents were commercially available. ^{1}H NMR and ^{13}C NMR spectra were obtained using a Bruker DRX spectrometer at 400 and 100 MHz respectively. Chemical shifts were reported in parts per million (ppm). Multiplicity of ^{1}H NMR signals was reported as singlet (s), doublet (d), triplet (t), quartert (q) and multiplet (m). ESI-MS data was recorded on an API 4000 spectrometer. High resolution mass spectra were conducted by Shandong Analysis and Test Center in Ji'nan. Melting points were determined on an electrothermal melting point apparatus and were uncorrected.

3,4-bis(phenylsulfonyl)-1,2,5-oxadiazole 2-oxide (**10**), 4-(4-hydroxybutoxy)-3-(phenylsulfonyl)-1,2,5-oxadiazole 2-oxide (**11a**), 4-((5-hydroxypentyl)oxy)-3-(phenylsulfonyl)-1,2,5-oxadiazole 2-oxide (**11b**), 4-((6-hydroxyhexyl)oxy)-3-(phenylsulfonyl)-1,2,5-oxadiazole 2-oxide (**11c**), 4-((7-hydroxyheptyl)oxy)-3-(phenylsulfonyl)-1,2,5-oxadiazole 2-oxide (**11d**), 4-((8-hydroxyoctyl)oxy)-3-(phenylsulfonyl)-1,2,5-oxadiazole 2-oxide (**11e**), 4-((9-hydroxynonyl)oxy)-3-(phenylsulfonyl)-1,2,5-oxadiazole 2-oxide (**11f**), 4-(4-(2-hydroxyethyl)phenoxy)-3-(phenylsulfonyl)-1,2,5-oxadiazole 2-oxide (**11g**), 4-(3-carboxypropoxy)-3-(phenylsulfonyl)-1,2,5-oxadiazole 2-oxide (**12a**), 4-(4-carboxybutoxy)-3-(phenylsulfonyl)-1,2,5-oxadiazole 2-oxide (**12b**), 4-((5-carboxypentyl)oxy)-3-(phenylsulfonyl)-1,2,5-oxadiazole 2-oxide (**12c**), 4-((6-carboxyhexyl)oxy)-3-(phenylsulfonyl)-1,2,5-oxadiazole 2-oxide (**12d**), 4-((7-carboxyheptyl)oxy)-3-(phenylsulfonyl)-1,2,5-oxadiazole 2-oxide (**12e**), 4-((8-carboxyoctyl)oxy)-3-(phenylsulfonyl)-1,2,5-oxadiazole 2-oxide (**12f**), 4-(4-(carboxymethyl)phenoxy)-3-(phenylsulfonyl)-1,2,5-

oxadiazole 2-oxide (**12g**), 4-(4-formylphenoxy)-3-(phenylsulfonyl)-1,2,5-oxadiazole 2-oxide (**13**), (E)-4-(4-(2-carboxyvinyl)phenoxy)-3-(phenylsulfonyl)-1,2,5-oxadiazole 2-oxide (**14**) were obtained as previously described [20].

4-(4-((2-aminophenyl)amino)-4-oxobutoxy)-3-(phenylsulfonyl)-1,2,5-oxadiazole 2-oxide (**7a**). At 0 ˚C, to a solution of compound **12a** (0.46 g, 1.4 mmol) in dried THF (30 mL), were added TBTU (0.53 g, 1.6 mmol) and TEA (0.28 mL, 2.0 mmol). After stirring for 40 min, *o*-phenylenediamine (0.17 g, 1.6 mmol) was added. The mixture was stirred for an additional 4 h at room temperature, then the solvent was removed under vacuum, with the residues being taken up in EtOAc. The organic portion was washed by water and brine, dried with anhydrous Na_2SO_4. The solvent was evaporated to get the crude product, which was purified by silica chromatography column (DCM/MeOH = 20:1) to obtain **7a** (0.29 g, 39% yield), white solid. Mp: 150 − 152℃. ^{1}H NMR (400 MHz, DMSO-d_6) δ 9.20 (s, 1H), 8.05 (d, J = 8.6 Hz, 2H), 7.89 (t, J = 4.0 Hz, 1H), 7.75 (t, J = 8.6 Hz, 2H), 7.17 (d, J = 9.0 Hz, 1H), 6.91 (t, J = 8.5 Hz, 1H), 6.73 (d, J = 9.1 Hz, 1H), 6.60 – 6.52 (m, 1H), 4.48 (t, J = 7.3 Hz, 2H), 2.08 (q, J = 7.5 Hz, 2H). ^{13}C NMR (101 MHz, DMSO-d_6) δ 170.66, 159.40, 142.50, 137.61, 136.62, 130.50, 128.87, 126.34, 125.99, 123.80, 122.99, 116.63, 116.32, 111.06, 71.46, 31.90, 24.60. HRMS (AP-ESI) m/z calcd for $C_{18}H_{19}N_4O_6S$ $[M + H]^+$: 419.1025; found: 419.0989.

Compounds **7b**-**7h** were prepared in a similar method as described for compound **7a**.

4-((5-((2-aminophenyl)amino)-5-oxopentyl)oxy)-3-(phenylsulfonyl)-1,2,5-oxadiazole 2-oxide (**7b**). White solid. 40% yield. Mp: 136-138℃. ^{1}H NMR (400 MHz, DMSO-d_6) δ 9.16 (s, 1H), 8.07–7.98 (m, 2H), 7.93–7.84 (m, 1H), 7.78–7.70 (m, 2H), 7.18 (dd, J = 7.8, 1.6 Hz, 1H), 6.91 (td, J = 7.6, 1.6 Hz, 1H), 6.73 (dd, J = 8.0, 1.5 Hz, 1H), 6.55 (td, J = 7.5, 1.5 Hz, 1H), 4.89 (s, 2H), 4.43 (t, J = 6.1 Hz, 2H), 2.40 (t, J = 7.2 Hz, 2H), 1.86–1.78 (m, 2H), 1.76–1.68 (m, 2H). ^{13}C NMR (101 MHz, DMSO-d_6) δ 171.28, 159.36, 142.41, 137.67, 136.61, 130.53, 128.81, 126.24, 125.78, 123.93, 116.64, 116.36, 110.93, 71.66, 35.48, 27.95, 21.89. HRMS (AP-ESI) m/z calcd for $C_{19}H_{21}N_4O_6S$ $[M + H]^+$: 433.1182; found: 433.1178.

4-((6-((2-aminophenyl)amino)-6-oxohexyl)oxy)-3-(phenylsulfonyl)-1,2,5-oxadiazole 2-oxide (**7c**). White solid. 35% yield. Mp: 129-131℃. ^{1}H NMR (400 MHz, DMSO-d_6) δ 9.36 (s, 1H), 8.01 (d, J = 7.9 Hz, 2H), 7.89 (t, J = 7.4 Hz, 1H), 7.74 (t, J = 7.7 Hz, 2H), 7.21 (d, J = 7.9 Hz, 1H), 6.97 (t, J = 7.5 Hz, 1H), 6.84 (d, J = 8.0 Hz, 1H), 6.69 (t, J = 7.5 Hz, 1H), 4.43–4.39 (m, 2H), 2.37 (t, J = 7.5 Hz, 2H), 1.85–1.74 (m, 2H), 1.70–1.62 (m, 2H), 1.46–1.39 (m, 2H). ^{13}C NMR (101 MHz, DMSO) δ 171.75, 159.36, 137.65, 136.61, 130.52, 128.77, 126.32, 125.93, 125.88, 119.59, 118.33, 110.92, 71.83, 36.01, 28.17, 25.23, 25.15. HRMS (AP-ESI) m/z calcd for $C_{20}H_{23}N_4O_6S$ $[M + H]^+$: 447.1338; found: 447.1328 .

4-((7-((2-aminophenyl)amino)-7-oxoheptyl)oxy)-3-(phenylsulfonyl)-1,2,5-oxadiazole 2-oxide (**7d**). White solid. 42% yield. Mp: 137-139℃. ^{1}H NMR (400 MHz, DMSO-d_6) δ 9.18 (s, 1H), 8.02 (d, J = 7.8 Hz, 2H), 7.90 (t, J = 7.4 Hz, 1H), 7.75 (t, J = 7.6 Hz, 2H), 7.17 (d, J = 7.8 Hz, 1H), 6.91 (t, J = 7.6 Hz, 1H), 6.75 (d, J = 8.0 Hz, 1H), 6.57 (t, J = 7.6 Hz, 1H), 4.39 (t, J = 6.3 Hz, 2H), 2.34 (t, J = 7.5 Hz, 2H), 1.80–1.73 (m, 2H), 1.66–1.58 (m, 2H), 1.38 (d, J = 7.0 Hz, 4H). ^{13}C NMR (101 MHz, DMSO-d_6) δ 171.65, 159.34, 141.41, 137.67, 136.60, 130.50, 128.76, 126.19, 125.77, 124.48, 117.34, 116.84, 110.90, 71.87, 36.13, 28.62, 28.21, 25.64, 25.30. HRMS (AP-ESI) m/z calcd for $C_{21}H_{25}N_4O_6S$ $[M + H]^+$: 461.1495; found: 461.1489

4-((8-((2-aminophenyl)amino)-8-oxooctyl)oxy)-3-(phenylsulfonyl)-1,2,5-oxadiazole 2-oxide (**7e**). White solid. 47% yield. Mp: 127-129℃. ^{1}H NMR (400 MHz, DMSO-d_6) δ 9.10 (s, 1H), 8.05–7.97 (m, 2H), 7.93–7.83 (m, 1H), 7.78–7.69 (m, 2H), 7.15 (dd, J = 7.9, 1.5 Hz, 1H), 6.89 (td, J = 7.6, 1.6 Hz, 1H), 6.71 (dd, J = 8.0, 1.5 Hz, 1H), 6.53 (td, J = 7.5, 1.5 Hz, 1H), 4.82 (s, 2H), 4.39 (t, J = 6.3 Hz, 2H), 2.33 (t, J = 7.4 Hz, 2H), 1.75 (t, J = 6.6 Hz, 2H), 1.65–1.57 (m, 2H), 1.38–1.33 (m, 6H). ^{13}C NMR (101 MHz, DMSO-d_6) δ 171.62, 159.35, 142.32, 137.70, 136.61, 130.50, 128.74, 126.14, 125.72, 124.06, 116.64, 116.36, 110.90, 71.93, 36.22, 29.21, 29.09, 28.92, 28.31, 25.77, 25.47. HRMS (AP-ESI) m/z calcd for $C_{22}H_{27}N_4O_6S$ $[M + H]^+$: 475.1651; found: 475.1633.

4-((9-((2-aminophenyl)amino)-9-oxononyl)oxy)-3-(phenylsulfonyl)-1,2,5-oxadiazole 2-oxide (**7f**). White solid. 33% yield. Mp: 130-132℃. ^{1}H NMR (400 MHz, DMSO-d_6) δ 9.09 (s, 1H), 8.01 (d, J = 7.9 Hz, 2H), 7.89 (t, J = 7.4 Hz, 1H), 7.75 (t, J = 7.6 Hz, 2H), 7.15 (d, J = 7.9 Hz, 1H), 6.88 (t, J = 7.6 Hz, 1H), 6.71 (d, J = 8.0 Hz, 1H), 6.53 (t, J = 7.6 Hz, 1H), 4.85 (s, 2H), 4.38 (t, J = 6.3 Hz, 2H), 2.32 (t, J = 7.3 Hz, 2H), 1.78–1.71 (m, 2H), 1.65–1.55 (m, 2H), 1.33 (s, 8H). ^{13}C NMR (101 MHz, DMSO-d_6) δ 171.63, 159.36, 142.31, 137.72, 136.60, 130.49, 128.74, 126.14, 125.72, 124.08, 116.66, 116.38, 110.90, 71.95, 36.24, 29.21, 29.09, 28.92, 28.32, 25.77, 25.48. HRMS (AP-ESI) m/z calcd for $C_{23}H_{29}N_4O_6S$ $[M + H]^+$: 489.1808; found: 489.1800.

4-(4-((2-aminophenyl)carbamoyl)phenoxy)-3-(phenylsulfonyl)-1,2,5-oxadiazole 2-oxide (**7g**). White solid. 30% yield. Mp: 180-182℃. ^{1}H NMR (400 MHz, DMSO-d_6) δ 9.73 (s, 1H), 8.08 (dd, J = 16.5, 8.1 Hz, 4H), 7.93 (t, J = 7.4 Hz, 1H), 7.78 (t, J = 7.7 Hz, 2H), 7.58 (d, J = 8.4 Hz, 2H), 7.17 (d, J = 7.9 Hz, 1H), 6.98 (t, J = 7.6 Hz, 1H), 6.78 (d, J = 8.0 Hz, 1H), 6.60 (t, J = 7.6 Hz, 1H), 4.95 (s, 2H). ^{13}C NMR (101 MHz, DMSO) δ 164.75, 158.53, 155.36, 143.80, 137.29, 136.78, 133.22, 130.52, 130.47, 129.10, 127.36, 127.14, 123.44, 119.73, 116.61, 116.47, 111.89. HRMS (AP-ESI) m/z calcd for $C_{21}H_{17}N_4O_6S$ $[M + H]^+$: 453.0869; found: 453.0861.

(*E*)-4-(4-(3-((2-aminophenyl)amino)-3-oxoprop-1-en-1-yl)phenoxy)-3-(phenylsulfonyl)-1,2,5-oxadiazole 2-oxide (**7h**). White solid. 47% yield. Mp: 168-170℃. ^{1}H NMR (400 MHz, DMSO-d_6) δ 9.41 (s, 1H), 8.05 (d, J = 7.8 Hz, 2H), 7.93 (t, J = 7.4 Hz, 1H), 7.84–7.71 (m, 4H), 7.64–7.45 (m, 3H), 7.35 (d, J = 7.9 Hz, 1H), 6.92 (q, J = 6.9 Hz, 2H), 6.76 (d, J = 8.0 Hz, 1H), 6.59 (t, J = 7.6 Hz, 1H), 4.95 (s, 2H). ^{13}C NMR (101 MHz, DMSO) δ 163.78, 158.63, 153.85, 142.10, 138.67, 137.34, 136.76, 133.75, 130.52, 129.85, 129.05, 126.32, 125.23, 123.88, 123.52, 120.63, 116.75, 116.47, 111.81. HRMS (AP-ESI) m/z calcd for $C_{23}H_{19}N_4O_6S$ $[M + H]^+$: 479.1025; found: 479.1004.

4.2. In vitro HDACs inhibition fluorescence assay

10 μL of enzyme solution (HeLa cell nuclear extract, HDAC1, HDAC2, HDAC3 or HDAC6) was mixed with different concentrations of tested compound (50 μL). The mixture was incubated at 37 ˚C for 5 mins, followed by adding 40 μL fluorogenic substrate (Boc-Lys(acetyl)-AMC for HeLa cell nuclear extract, HDAC1, HDAC2, HDAC3 and HDAC6, Boc-Lys(trifluoroacetyl)-AMC for HDAC4). After incubation at 37 ˚C for 30 mins, the mixture was quenched by addition of 100 μL of developer containing trypsin and Trichostatin A. Over another incubation at 37 ˚C for 20 min, fluorescence intensity was measured using a microplate reader at excitation and emission wavelengths of 390 and 460 nm, respectively. The inhibition ratios were calculated from the fluorescence intensity readout of tested wells relative to those of control wells, and the IC_{50} values were calculated using Prism non-linear curve fitting method.

4.3. In vitro NO measurement

The in vitro NO measurement was tested using the Griess method [24]. The level of NO generated by individual compound in the cells was presented as that of nitrite and determined by the colorimetric assay using the colorimetric assay kit (purchased from Beyotime, China), according to the manufacturer's instruction. Briefly, HeLa cells (5×10^5/well) were treated with a 10 μM of tested compounds for 1 h or 5 h. Subsequently, the cells were harvested, and their cell lysates were prepared and then mixed with Griess for 10 min at 37℃, followed by measurement at 540 nm by an enzyme-linked immunosorbent assay plate reader. The cells treated with DMSO were used as negative

controls for the background level of nitrite production, while sodium nitrite at different concentrations was prepared for the standard curve.

4.4. Western blot analysis

For regular western blot analysis, the HeLa cells were treated with MS275 (2 μM), **7c** (2 μM) or DMSO for 5 h. For western blot analysis to investigate if NO generated by **7c** contributed to its intracellular HDAC inhibition, the HeLa cells were preincubated with 10 μM of NAC, then were treated with 2 μM of MS275 or **7c** for 5 h. After treatment, the cells were washed twice with cold PBS and lysed in ice-cold RIPA buffer. Lysates were cleared by centrifugation. Protein concentrations were determined using the BCA assay. Equal amounts of cell extracts were then resolved by SDS-PAGE, transferred to nitrocellulose membranes and probed with ac-histone H4 antibody, ac-α-tubulin antibody and β-actin antibody, respectively. Blots were detected using an enhanced chemiluminescence system.

4.5. In vitro anti-proliferative assay

All cell lines were maintained in RPMI1640 medium containing 10% FBS at 37℃ in a 5% CO_2 humidified incubator. Cell proliferation assay was determined by the MTT (3-[4,5-dimethyl-2-thiazolyl]-2,5-diphenyl-2 h-tetrazolium bromide) method. Briefly, cells were passaged the day before dosing into a 96-well plate, allowed to grow for 12 h, and then treated with different concentrations of compound for 48 h. A 0.5% MTT solution was added to each well. After incubation for another 4 h, formazan formed from MTT was extracted by adding 200 uL of DMSO. Absorbance was then determined using an ELISA reader at 570 nm.

4.6. In vivo antitumor experiment in HCT116 xenograft model

All experiments involving laboratory animals were performed with the approval of local ethics committee for animal experimentation. In vivo human tumor xenograft models were established as previously described [25,26]. In brief, 1×10^7 HCT 116 cells were inoculated subcutaneously in the right flank of male athymic nude mice (BALB/c-nu, 5–6 weeks old, Beijing HFK Bioscience Co., Ltd.). Ten days after injection, tumors were palpable and mice were randomized into treatment and control groups (5 mice per group). The treatment groups received compound **7c** or MS275 by oral administration (30 mg/kg/d), and the blank control group received oral administration of equal volume of PBS (5% DMSO). Subcutaneous tumors were measured with a vernier caliper every three days. Tumor volumes (V) were estimated using the equation ($V = ab^2/2$, where a and b stand for the longest and shortest diameter, respectively). Mice body weight was also monitored regularly. At the end of experimental period, mice were sacrificed and dissected to weigh the tumor tissues. Tumor growth inhibition (TGI) and relative increment ratio (T/C) were calculated at the end of treatment to reveal the antitumor effects in tumor weight and tumor volume, respectively.

TGI = (the mean tumor weight of control group - the mean tumor weight of treated group)/the mean tumor weight of control group.

T/C = the mean RTV of treated group (T) / the mean RTV of blank control group (C).

RTV, namely relative tumor volume, is V_t/V_0 (V_t: the tumor volume measured at the end of treatment; V_0: the tumor volume measured at the beginning of the treatment).

All the obtained data were used to evaluate the antitumor potency and toxicity of compounds. Data were analyzed by Student's two-tailed *t* test. A p-value of < 0.05 was considered statistically significant.

Declaration of Competing Interest

The authors declare that they have no known competing financial interests or personal relationships that could have appeared to influence the work reported in this paper.

Acknowledgement

This work was supported by Natural Science Foundation of Shandong Province (Grant No. ZR2018QH007), Key Research and Development Program of Shandong Province (2017CXGC1401), Young Scholars Program of Shandong University (YSPSDU, 2016WLJH33).

Appendix A. Supplementary data

Supplementary data to this article can be found online at https://doi.org/10.1016/j.bioorg.2020.104235.

References

[1] R. Sangwan, R. Rajan, P.K. Mandal, HDAC as onco target: Reviewing the synthetic approaches with SAR study of their inhibitors, Eur. J. Med. Chem. 158 (2018) 620–706.
[2] C. Zagni, G. Floresta, G. Monciino, A. Rescifina, The search for potent, small-molecule HDACIs in cancer treatment: a decade after Vorinostat, Med. Res. Rev. 37 (2017) 1373–1428.
[3] D. Tomaselli, A. Lucidi, D. Rotili, A. Mai, Epigenetic polypharmacology: A new frontier for epi-drug discovery, Med Res Rev 40 (2020) 190–244.
[4] M. Guha, HDAC inhibitors still need a home run, despite recent approval, Nat. Rev. Drug Discov. 14 (2015) 225–226.
[5] Y.Y. Juo, X.J. Gong, A. Mishra, X. Cui, S.B. Baylin, N.S. Azad, N. Ahuja, Epigenetic therapy for solid tumors: from bench science to clinical trials, Epigenomics 7 (2015) 215–235.
[6] J.H. Kalin, M. Wu, A.V. Gomez, Y. Song, J. Das, D. Hayward, N. Adejola, M. Wu, I. Panova, C.H. J., E. Kim, H.J. Roberts, J.M. Roberts, P. Prusevich, J.R. Jeliazkov, S.S. Roy Burman, L. Fairall, C. Milano, A. Eroglu, C.M. Proby, A.T. Dinkova-Kostova, W. W. Hancock, J.J. Gray, J.E. Bradner, S. Valente, A. Mai, N.M. Anders, M.A. Rudek, Y. Hu, B. Ryu, J.W.R. Schwabe, A. Mattevi, R.M. Alani, P.A. Cole, Targeting the CoREST complex with dual histone deacetylase and demethylase inhibitors, Nat. Commun., 9 (2018) 53.
[7] G. Dong, W. Chen, X. Wang, X. Yang, T. Xu, P. Wang, W. Zhang, Y. Rao, C. Miao, C. Sheng, Small molecule inhibitors simultaneously targeting cancer metabolism and epigenetics: discovery of novel nicotinamide phosphoribosyltransferase (NAMPT) and histone deacetylase (HDAC) dual inhibitors, J. Med. Chem. 60 (2017) 7965–7983.
[8] Y. Ling, C. Xu, L. Luo, J. Cao, J. Feng, Y. Xue, Q. Zhu, C. Ju, F. Li, Y. Zhang, Novel β-carboline/hydroxamic acid hybrids targeting both histone deacetylase and DNA display high anticancer activity via regulation of the p53 signaling pathway, J. Med. Chem. 58 (2015) 9214–9227.
[9] L.M. López-Sánchez, E. Aranda, A. Rodríguez-Ariza, Nitric oxide and tumor metabolic reprogramming, Biochem. Pharmacol. 176 (2020) 113769.
[10] C. Szabo, Gasotransmitters in cancer: from pathophysiology to experimental therapy, Nat. Rev. Drug Discov 15 (2016) 185–203.
[11] B. Bonavida, Sensitizing activities of nitric oxide donors for cancer resistance to anticancer therapeutic drugs, Biochem. Pharmacol. 176 (2020) 113913.
[12] Z. Huang, J. Fu, Y. Zhang, Nitric Oxide Donor-Based Cancer Therapy: Advances and Prospects, J. Med. Chem. 60 (2017) 7617–7635.
[13] O. Arrieta, M. Blake, M. de la Mata-Moya, F. Corona, J. Turcott, D. Orta, J. Alexander-Alatorre, D. Gallardo-Rincón, Phase II study. Concurrent chemotherapy and radiotherapy with nitroglycerin in locally advanced non-small cell lung cancer, Radiother. Oncol. 111 (2014) 311–315.
[14] H. Yasuda, M. Yamaya, K. Nakayama, T. Sasaki, S. Ebihara, A. Kanda, M. Asada, D. Inoue, T. Suzuki, T. Okazaki, H. Takahashi, M. Yoshida, T. Kaneta, K. Ishizawa, S. Yamanda, N. Tomita, M. Yamasaki, A. Kikuchi, H. Kubo, H. Sasaki, Randomized phase II trial comparing nitroglycerin plus vinorelbine and cisplatin with vinorelbine and cisplatin alone in previously untreated stage IIIB/IV non-small-cell lung cancer, J. Clin. Oncol. 24 (2006) 688–694.
[15] H. Zhao, S. Ning, J. Scicinski, B. Oronsky, S. Knox, D.M. Peehl, RRx-001: A double action systemically non-toxic epigenetic agent for cancer therapy, Cancer Res. 75 (2015) 3515.
[16] T. Reid, S. Dad, R. Korn, B. Oronsky, S. Knox, J. Scicinski, Two case reports of resensitization to previous chemotherapy with the novel hypoxia-activated hypomethylating anticancer agent RRx-001 in metastatic colorectal cancer patients, Case Rep. Oncol. 7 (2014) 79–85.
[17] A. Nott, P.M. Watson, J.D. Robinson, L. Crepaldi, A. Riccio, S-Nitrosylation of histone deacetylase 2 induces chromatin remodelling in neurons, Nature 455 (2008) 411–415.
[18] A. Nott, J. Nitarska, J.V. Veenvliet, S. Schacke, A.A.H.A. Derijck, P. Sirko, C. Muchardt, R.J. Pasterkamp, M.P. Smidt, A. Riccio, S-nitrosylation of HDAC2

regulates the expression of the chromatin-remodeling factor Brm during radial neuron migration, Proc. Natl. Acad. Sci. USA 110 (2013) 3113–3118.
[19] C. Colussi, C. Mozzetta, A. Gurtner, B.R. Illi, J., S. Straino, G. Ragone, M. Pescatori, G. Zaccagnini, A. Antonini, G. Minetti, F. Martelli, G. Piaggio, P. Gallinari, C. Steinkuhler, E. Clementi, C. Dell'Aversana, L. Altucci, A. Mai, M.C. Capogrossi, P.L. Puri, C. Gaetano, HDAC2 blockade by nitric oxide and histone deacetylase inhibitors reveals a common target in Duchenne muscular dystrophy treatment, Proc. Natl. Acad. Sci. USA, 105 (2008) 19183–19187.
[20] W. Duan, J. Li, E.S. Inks, C. James Chou, Y. Jia, X. Chu, X. Li, W. Xu, Y. Zhang, Design, Synthesis, and Antitumor Evaluation of Novel Histone Deacetylase Inhibitors Equipped with a Phenylsulfonylfuroxan Module as a Nitric Oxide Donor, J. Med. Chem. 58 (2015) 4325–4338.
[21] M. Borgini, C. Zamperini, F. Poggialini, L. Ferrante, V. Summa, M. Botta, R.D. Fabio, Synthesis and Antiproliferative Activity of Nitric Oxide-Donor Largazole Prodrugs, ACS Med. Chem. Lett. 11 (2020) 846–851.
[22] S. Atlante, K. Chegaev, C. Cencioni, S. Guglielmo, E. Marini, E. Borretto, C. Gaetano, R. Fruttero, F. Spallotta, L. Lazzarato, Structural and biological characterization of new hybrid drugs joining an HDAC inhibitor to different NO-donors, Eur. J. Med. Chem. 144 (2018) 612–625.
[23] E. Borretto, L. Lazzarato, F. Spallotta, C. Cencioni, Y. D'Alessandra, C. Gaetano, R. Fruttero, A. Gasco, Synthesis and Biological Evaluation of the First Example of NO-Donor Histone Deacetylase Inhibitor, ACS Med. Chem. Lett 4 (2013) 994–999.
[24] N.S. Bryan, M.B. Grisham, Methods to detect nitric oxide and its metabolites in biological samples, Free Radical Biol. Med. 43 (2007) 645–657.
[25] X. Li, Y. Zhang, Y. Jiang, J. Wu, E.S. Inks, C. James Chou, S. Gao, J. Hou, Q. Ding, J. Li, X. Wang, Y. Huang, W. Xu, Selective HDAC inhibitors with potent oral activity against leukemia and colorectal cancer: Design, structure-activity relationship and anti-tumor activity study, Eur. J. Med. Chem. 134 (2017) 185–206.
[26] Y. Zhang, H. Fang, J. Feng, Y. Jia, X. Wang, W. Xu, Discovery of a Tetrahydroisoquinoline-Based Hydroxamic Acid Derivative (ZYJ-34c) as Histone Deacetylase Inhibitor with Potent Oral Antitumor Activities, J. Med. Chem. 54 (2011) 5532–5539.